Imaging Science in Dentistry 2023; 53: 43-51
https://doi.org/10.5624/isd.20220166

Cone-beam computed tomography texture analysis can help differentiate odontogenic and non-odontogenic maxillary sinusitis

Andre Luiz Ferreira Costa[1,*], Karolina Aparecida Castilho Fardim[2], Isabela Teixeira Ribeiro[2], Maria Aparecida Neves Jardini[2], Paulo Henrique Braz-Silva[3,4], Kaan Orhan[5], Sérgio Lúcio Pereira de Castro Lopes[2]

[1]*Postgraduate Program in Dentistry, Cruzeiro do Sul University, São Paulo, SP, Brazil*
[2]*Department of Diagnosis and Surgery, São José dos Campos School of Dentistry of the São Paulo State University, São José dos Campos, SP, Brazil*
[3]*Division of General Pathology, School of Dentistry, University of São Paulo, São Paulo, SP, Brazil*
[4]*Laboratory of Virology, Institute of Tropical Medicine of São Paulo, School of Medicine, University of São Paulo, São Paulo, SP, Brazil*
[5]*Department of Dentomaxillofacial Radiology, Faculty of Dentistry, Ankara University, Ankara, Turkey*

ABSTRACT

Purpose: This study aimed to assess texture analysis (TA) of cone-beam computed tomography (CBCT) images as a quantitative tool for the differential diagnosis of odontogenic and non-odontogenic maxillary sinusitis (OS and NOS, respectively).

Materials and Methods: CBCT images of 40 patients diagnosed with OS (N = 20) and NOS (N = 20) were evaluated. The gray level co-occurrence (GLCM) matrix parameters, and gray level run length matrix texture (GLRLM) parameters were extracted using manually placed regions of interest on lesion images. Seven texture parameters were calculated using GLCM and 4 parameters using GLRLM. The Mann-Whitney test was used for comparisons between the groups, and the Levene test was performed to confirm the homogeneity of variance ($\alpha = 5\%$).

Results: The results showed statistically significant differences ($P < 0.05$) between the OS and NOS patients regarding 3 TA parameters. NOS patients presented higher values for contrast, while OS patients presented higher values for correlation and inverse difference moment. Greater textural homogeneity was observed in the OS patients than in the NOS patients, with statistically significant differences in standard deviations between the groups for correlation, sum of squares, sum of entropy, and entropy.

Conclusion: TA enabled quantitative differentiation between OS and NOS on CBCT images by using the parameters of contrast, correlation, and inverse difference moment. ***(Imaging Sci Dent 2023; 53: 43-51)***

KEY WORDS: Cone-Beam Computed Tomography; Diagnosis, Computer-Assisted; Diagnostic Imaging; Paranasal Sinuses

Introduction

The maxillary sinuses are considered the largest paranasal sinuses in the maxilla, being the first to develop in the region between the orbital and nasal cavities. Inflammation of the membrane lining this cavity, the sinus membrane, is referred to as sinusitis, the main etiology of which involves alterations in the nasal cavities; sinusitis of this etiology is known as non-odontogenic sinusitis (NOS). However, in some cases, sinusitis may have an etiology of dental origin, in which case it is called odontogenic sinusitis (OS).[1]

The proximity between the roots of posterior teeth and the floor of the maxillary sinuses, in combination with the presence of infectious and inflammatory processes of odontogenic origin (e.g. periapical lesions), can affect the integrity of this floor, causing inflammatory changes in the mucous lining and subsequently leading to the development of OS.[2] The literature states that iatrogenic (65%) and apical peri-

This study was supported by The São Paulo Research Foundation (FAPESP) n° 2020/08295-3 and n° 2019/00495-6.
Received September 22, 2022; Revised December 2, 2022; Accepted December 14, 2022
Published online January 11, 2023
*Correspondence to : Prof. Andre Luiz Ferreira Costa
Postgraduate Program in Dentistry, Cruzeiro do Sul University, Rua Galvão Bueno, 868, Liberdade, São Paulo, SP 01506-000, Brazil
Tel) 55-11-33853015, E-mail) alfcosta@gmail.com

odontitis (i.e., periapical inflammatory lesions) (16.8%), mainly in the molars, are the main causes of OS in the maxillary sinuses.[3]

The symptoms of OS are similar to those observed in NOS, such as nasal obstruction or congestion with the presence of yellowish secretions, pain or pressure on the face, headaches increasing in intensity with head movement, sensitivity in the anterior region and infra-orbital region of the maxilla, eye pain, post-nasal drip, and bad odor.[4] However, despite the similar symptomatology, OS and NOS should be carefully differentiated since these conditions have distinct microbiology, pathophysiology, and management.[4,5]

For an accurate diagnosis of both pathologies to facilitate an appropriate intervention, close collaboration between dentists and otolaryngologists is essential.[5]

Cone-beam computed tomography (CBCT) has been widely used as a complementary imaging technique to evaluate the paranasal sinuses. On CBCT images, the maxillary sinus content usually appears completely hypodense with defined bony margins. Cloudiness in the sinus, revealing opacification, indicates the presence of mucosal thickening causing near-complete occlusion.[6,7]

Imaging methodologies are well understood and have been used, in addition to anatomopathological analysis, to differentiate OS from NOS.[2,8] However, the absence of teeth in the region of analysis of CBCT images, or even the reduced field of view (FOV) during image acquisition, can sometimes make it impossible to use this approach for differentiation. Thus, a more independent methodology based only on sinus content, which would allow an objective assessment, would be very valuable for the differential diagnosis between OS and NOS.

In this context, because of the difference in the microbiota between OS and NOS,[9] images indicating the presence of maxillary sinusitis (i.e., opacification) may show differences in the degree of X-ray attenuation between these conditions, which could help in the differential diagnosis using CBCT exams. However, this fact is not subjectively perceptible during image analysis, often raising doubts about the type of sinusitis in question, which can influence the conduct and success of treatment. Thus, a method for quantitative analysis capable of deriving numerical and statistically analyzable data from CBCT images of maxillary sinusitis would enable the differentiation between OS and NOS, which would be very valuable as an auxiliary diagnostic tool.

With advances in digital image processing and computer-assisted diagnosis techniques, a post-processing methodology for quantifying complex structures in images more efficiently and less invasively was developed, in which the distribution of gray levels in a region of interest (ROI) on the image is measured for texture analysis (TA).[10-12]

Texture parameters are computed mathematical properties over a pixel distribution, which characterizes the type of texture and structure of the objects shown in the image but are imperceptible to the human eye.[13,14] The different methods for performing TA are usually classified depending on the approach used to extract parameters representative of the image texture.[15,16]

Previous studies have used TA to characterize lesions in various regions of the body and to distinguish them from normal tissues, with greater heterogeneity of texture parameters being observed in pathological tissues.[17-19]

In dentistry, TA has been applied to help with the clinical interpretation of several types of lesions, such as caries, granuloma, radicular cyst, and furcal lesion.[13,20,21]

TA can be understood as the analysis of a set of intrinsic image properties related to the appearance, structure, and arrangement of the various parts of the object selected. These characteristics are extracted from signal patterns of pixels or voxels imperceptible to the human eye.[13,14,16]

Therefore, this study aimed to evaluate the use of the technique of TA in CBCT images as a tool to improve the differential diagnosis between OS and NOS in the maxillary sinuses.

Materials and Methods

Sample

This retrospective study was approved by the Research Ethics Committee of the School of Dentistry of São José dos Campos, UNESP, according to protocol 34235020.0.0000.0077.

The sample consisted of 250 CBCT images acquired from December 2019 to December 2020, all obtained from the database of the Oral Radiology Department of the School of Dentistry of São José dos Campos, UNESP. This study's sample included subjects who underwent CBCT scanning for planning implant or endodontic treatment.

The CBCT images were acquired by using a scanning unit (OP300 Maxio, Instrumentarium Dental, Tuusula, Finland) with the following acquisition parameters: 90 kVp, 12.5 mA, voxel size of 0.085 mm, FOV of 5.0 × 5.0 cm and acquisition time of 8.7 s. All images were obtained in the Digital Imaging and Communications in Medicine (DICOM) format.

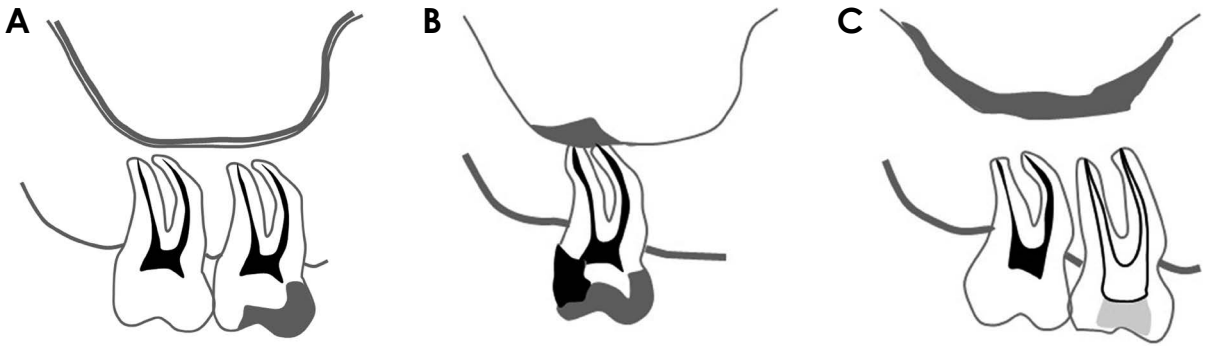

Fig. 1. Diagrams show cone-beam computed tomographic images of the maxillary sinus. A. Normal content of the maxillary sinus. B. Odontogenic sinusitis. C. Non-odontogenic sinusitis.

Imaging data

The imaging-based diagnostic criteria used in the present study for sinusitis diagnosis were adapted from elsewhere[2] as follows. First, a normal sinus was defined as the absence of any soft tissue density content or uniform mucosal thickening less than 2.00 mm thick; adjacent teeth are sound, without carious lesions, areas of pulp exposure, or restorations; if restorations are present, they have aspects of normality (Fig. 1A). Second, OS was defined as the presence of soft tissue density content with an average thickness above 2.00 mm inside the maxillary sinus and adjacent to the maxillary sinus floor, being restricted to the region of a tooth with a close relationship with its root apex or apices and the corresponding maxillary sinus floor. This tooth should have carious lesions with pulp involvement, extensively fractured restorations, and/or periapical lesions in contact with the sinus floor, and not be endodontically treated (Fig. 1B). Third, NOS was defined as the presence of soft tissue density content with an average thickness above 2.00 mm inside the maxillary sinus, which may extend to the sinus floor, and teeth in the region with no close relationship with its root apex(s) and corresponding maxillary sinus floor. These teeth should not have carious lesions with pulp involvement and periapical lesions, and if carried out, endodontic treatment should be satisfactory (Fig. 1C).

Patients with maxillofacial trauma, a history of paranasal sinus surgery, images with impaired visualization of the details, or images containing artifacts, all of which make it difficult to visualize anatomical structures, were excluded from the study.

Without knowing the clinical information and without viewing any other images, 2 oral radiologists with experience in CBCT imaging diagnosis reviewed and analyzed all the images together to select and identify sinusitis. After reviewing the images, the final sample consisted of 40 subjects with maxillary sinusitis, of whom 20 had odontogenic sinusitis (OS group) and 20 had non-odontogenic sinusitis (NOS group).

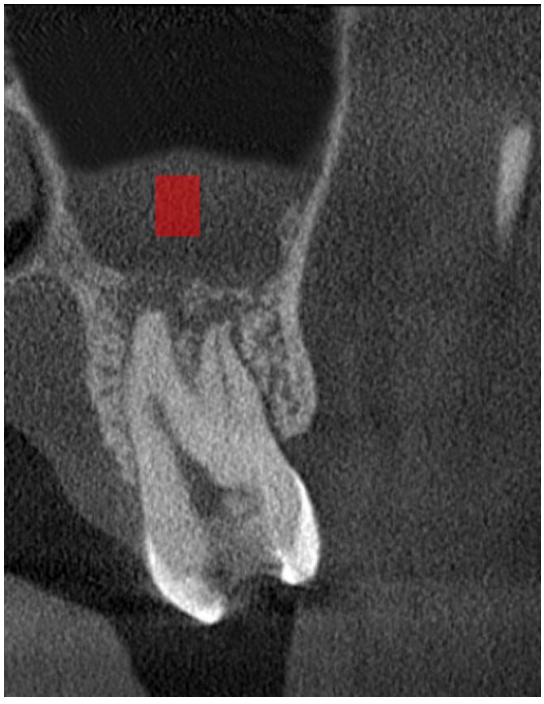

Fig. 2. Sagittal cone-beam computed tomographic image shows a region of interest for analysis of the maxillary sinus using the MaZda software.

Texture analysis

All DICOM datasets were imported into OnDemand3D software (CyberMed Inc., Seoul, Korea) and a single operator (a dentomaxillofacial radiologist with 5 years of experience) analyzed the images on a 19-inch LCD widescreen monitor (Samsung, Seoul, Korea). In a cross-sectional view, the 3 most central image slices per patient were chosen,

Table 1. Texture parameter selection using the gray level co-occurrence matrix method for the analysis of non-odontogenic sinusitis and odontogenic sinusitis groups

Positions/parameter	Non-odontogenic sinusitis (N = 20)	Odontogenic sinusitis (N = 20)
S(1.0)AngScMom	0.12 [0.03;0.63]	0.16 [0.01;0.37]
S(0.1)AngScMom	0.14 [0.03;0.63]	0.16 [0.01;0.39]
S(2.0)AngScMom	0.09 [0.02;0.58]	0.11 [0.01;0.32]
S(0.2)AngScMom	0.10 [0.02;0.58]	0.11 [0.01;0.32]
S(3.0)AngScMom	0.08 [0.02;0.55]	0.10 [0.01;0.29]
S(0.3)AngScMom	0.09 [0.02;0.55]	0.10 [0.01;0.29]
S(1.0)Contrast	0.68 [0.10;3.06]	0.33 [0.12;6.04]*
S(0.1)Contrast	0.44 [0.08;2.22]	0.32 [0.14;2.96]
S(2.0)Contrast	1.48 [0.18;7.05]	0.67 [0.24;19.8]*
S(0.2)Contrast	1.03 [0.14;5.62]	0.76 [0.28;9.72]
S(3.0)Contrast	2.12 [0.23;8.00]	1.02 [0.34;34.5]
S(0.3)Contrast	1.50 [0.18;7.15]	1.27 [0.40;17.3]
S(1.0)Correlat	0.70 [0.62;0.84]	0.83 [0.59;0.98]*
S(0.1)Correlat	0.80 [0.72;0.86]	0.87 [0.73;0.98]*
S(2.0)Correlat	0.38 [0.12;0.66]	0.62 [0.20;0.97]*
S(0.2)Correlat	0.53 [0.29;0.71]	0.69 [0.51;0.93]*
S(3.0)Correlat	0.09 [−0.27;0.46]	0.44 [−0.09;0.97]*
S(0.3)Correlat	0.27 [0.09;0.54]	0.51 [0.35;0.85]*
S(1.0)SumOfSqs	1.03 [0.16;4.00]	1.53 [0.34;17.3]
S(0.1)SumOfSqs	1.03 [0.17;3.93]	1.53 [0.33;16.3]
S(2.0)SumOfSqs	1.02 [0.15;4.01]	1.51 [0.34;17.8]
S(0.2)SumOfSqs	1.01 [0.17;3.97]	1.53 [0.33;16.7]
S(3.0)SumOfSqs	1.02 [0.15;3.99]	1.48 [0.34;18.2]
S(0.3)SumOfSqs	0.99 [0.17;3.92]	1.49 [0.32;17.1]
S(1.0)InvDfMom	0.74 [0.50;0.95]	0.85 [0.39;0.94]*
S(0.1)InvDfMom	0.80 [0.53;0.96]	0.85 [0.48;0.93]
S(2.0)InvDfMom	0.61 [0.35;0.91]	0.76 [0.24;0.88]*
S(0.2)InvDfMom	0.67 [0.38;0.93]	0.73 [0.31;0.86]
S(3.0)InvDfMom	0.55 [0.34;0.88]	0.69 [0.19;0.83]
S(0.3)InvDfMom	0.61 [0.34;0.91]	0.66 [0.23;0.81]
S(1.0)SumEntrp	0.88 [0.34;1.16]	0.87 [0.57;1.46]
S(0.1)SumEntrp	0.88 [0.34;1.17]	0.86 [0.55;1.48]
S(2.0)SumEntrp	0.84 [0.37;1.08]	0.86 [0.57;1.42]
S(0.2)SumEntrp	0.85 [0.38;1.11]	0.88 [0.59;1.47]
S(3.0)SumEntrp	0.78 [0.37;1.05]	0.83 [0.51;1.34]
S(0.3)SumEntrp	0.81 [0.40;1.07]	0.85 [0.58;1.45]
S(1.0)Entropy	1.09 [0.37;1.70]	0.98 [0.62;2.11]
S(0.1)Entropy	1.03 [0.37;1.64]	0.96 [0.59;2.00]
S(2.0)Entropy	1.20 [0.43;1.79]	1.13 [0.68;2.29]
S(0.2)Entropy	1.16 [0.42;1.77]	1.11 [0.68;2.21]
S(3.0)Entropy	1.23 [0.44;1.79]	1.20 [0.72;2.31]
S(0.3)Entropy	1.19 [0.45;1.77]	1.18 [0.71;2.30]

*: $P<0.05$, AngScMom: angular second moment, Correlat: correlation, InvDfMom: inverse difference moment, SumEntrp: sum of entropy; SumOfSqs: sum of squares

as sinusitis was more apparent or larger. These 3 image slices were used to increase the amount of data available in the CBCT volume to be used for TA.

The image slices selected were saved in .bmp format

and opened with MaZda software (Institute of Electronics, Lodz University of Technology, http://www.eletel.p.lodz.pl/mazda/). By using the draw rectangle tool, the operator manually determined a rectangular ROI (5.0 × 3.0 mm) for all images and positioned in the central region of the sinus opacification (Fig. 2).

In total, 11 parameters were computed for each ROI based on 2 of the 6 TA methods available in the MaZda software. The first method was the gray level co-occurrence matrix (GLCM), which provides information on the spatial relationship between the image's pixels contained in the ROI, as determined by the operator;[22] the parameters (i.e., second angular moment, contrast, correlation, entropy, inverse difference moment, sum of entropy, sum of squares) can be calculated for different positions determined by 2 distances between pixels (d1 = 1, d2 = 2) and by 4 image directions (i.e. horizontal, diagonal, vertical and anti-diagonal, corresponding to horizontal, vertical, 45° and 135°, respectively). The 2 distances can be arranged in the 4 directions in the following positions, namely: S(1.0), S(0.1); S(2.0), S(0.2); and S(3.0), S(0.3).[13] The second method was the gray level run length matrix (GLRLM), which represents runs of pixels having the same gray level value;[23] the chosen parameters (i.e., short-run emphasis, gray level non-uniformity, long-run emphasis, and run-length non-uniformity) can be arranged in horizontal and vertical directions.[15]

Statistical analysis

Comparisons between the groups were performed using the Mann-Whitney test, whereas the Levene test was performed to confirm the homogeneity of variance. The level of significance adopted was 5%. Statistical analysis was performed with the R software, version 4.1.0 (R Foundation for Statistical Computing, Vienna, Austria).

Results

The ages of the patients studied ranged from 25 to 51 years old. The mean age was 37.1 ± 7.9 years in the NOS group and 39 ± 7.0 years in the OS group. There was no statistically significant difference between the groups regarding age ($P > 0.05$) and sex ($P > 0.05$), as women made up 50% of the NOS group and 55% of the OS group.

Table 1 shows a comparison between the OS and NOS groups regarding the texture parameters analyzed in this study using GLCM. Statistically significant differences were found between the groups for 3 parameters of TA: 1) contrast, in the positions S(1.0) and S(2.0) for the NOS group ($P < 0.05$); 2) correlation, in all positions for the OS group ($P < 0.05$); and 3) moment of inverse difference, in the positions S(1.0) and S(2.0) for the OS ($P < 0.05$).

Table 2 shows the results of the comparison between the NOS and OS groups regarding variations in the vertical and horizontal directions for the selection of GLRLM parameters. Significantly higher differences were observed between the groups regarding vertical ($P < 0.05$) and horizontal ($P < 0.05$) directions, thus showing the capability of discriminating between NOS and OS.

Table 3 shows a comparison between the NOS and OS groups regarding the homogeneity of TA parameters using the Levene test. As shown in Table 3, the OS group showed greater homogeneity (lowest standard deviation) in the cor-

Table 2. Texture parameter selection using the gray level run length matrix method in the analysis of non-odontogenic sinusitis and odontogenic sinusitis groups

Directions/parameter	Non-odontogenic sinusitis (N = 20)	Odontogenic sinusitis (N = 20)
Horzl_RLNonUni	119 [7,16;318]	45,4 [11,4;365]*
Horzl_GLevNonU	81,8 [35,4;97,3]	49,3 [25,2;77,1]*
Horzl_LngREmph	5,80 [2,20;115]	13,6 [1,83;53,6]
Horzl_ShrtREmp	0,59 [0,16;0,81]	0,43 [0,15;0,88]
Horzl_Fraction	0,51 [0,12;0,75]	0,34 [0,17;0,82]
Vertl_RLNonUni	80,2 [7,84;298]	41,8 [12,5;317]*
Vertl_GLevNonU	73,2 [42,3;82,3]	39,4 [19,7;58,3]*
Vertl_LngREmph	9,03 [2,29;105]	18,0 [2,07;64,5]*
Vertl_ShrtREmp	0,49 [0,23;0,79]	0,43 [0,08;0,84]
Vertl_Fraction	0,42 [0,13;0,74]	0,32 [0,16;0,78]

*: $P < 0.05$, ShrtREmp: short run emphasis, GLevNonU: gray level non-uniformity, LngREmph: long run emphasis, RLNonUni: run-length non-uniformity, Horzl : Horizontal, Vertl: vertical

Table 3. Standard deviation calculated with the Levene test for each parameter using the gray level co-occurrence matrix and gray level run length matrix methods in the non-odontogenic sinusitis and odontogenic sinusitis groups

Parameter	Non-odontogenic sinusitis	Odontogenic sinusitis	Parameter	Non-odontogenic sinusitis	Odontogenic sinusitis
S10AngScMom	0.11	0.13	S02SumEntrp	0.27	0.15*
S10Contrast	1.51	0.62	S02Entropy	0.43	0.28
S10Correlat	0.11	0.06*	S30AngScMom	0.08	0.11
S10SumOfSqs	5.49	0.78*	S30Contrast	8.72	1.72
S10InvDfMom	0.14	0.10	S30Correlat	0.35	0.19*
S10SumEntrp	0.28	0.17*	S30SumOfSqs	5.66	0.78*
S10Entropy	0.41	0.28	S30InvDfMom	0.18	0.12
S01AngScMom	0.12	0.13	S30SumEntrp	0.25	0.13*
S01Contrast	0.76	0.43	S30Entropy	0.45	0.28
S01Correlat	0.07	0.04*	S03AngScMom	0.09	0.11
S01SumOfSqs	5.26	0.77*	S03Contrast	4.40	1.44
S01InvDfMom	0.12	0.09	S03Correlat	0.17	0.12
S01SumEntrp	0.28	0.17*	S03SumOfSqs	5.00	0.77*
S01Entropy	0.40	0.25	S03InvDfMom	0.16	0.12
S20AngScMom	0.09	0.12	S03SumEntrp	0.26	0.14*
S20Contrast	4.97	1.46	S03Entropy	0.45	0.27*
S20Correlat	0.23	0.15*	Horzl_RLNonUni	101.73	72.15
S20SumOfSqs	5.58	0.79*	Horzl_GLevNonU	16.99	15.30
S20InvDfMom	0.17	0.12	Horzl_LngREmph	14.00	24.72
S20SumEntrp	0.26	0.14*	Horzl_ShrtREmp	0.20	0.16
S20Entropy	0.45	0.29	Horzl_Fraction	0.18	0.15
S02AngScMom	0.10	0.12	Vertl_RLNonUni	86.46	62.54
S02Contrast	2.52	1.13	Vertl_GLevNonU	10.78	10.25
S02Correlat	0.13	0.10	Vertl_LngREmph	18.17	22.36
S02SumOfSqs	5.13	0.78*	Vertl_ShrtREmp	0.20	0.15
S02InvDfMom	0.16	0.11	Vertl_Fraction	0.17	0.13

*: $P<0.05$, AngScMom: angular second moment, Correlat: correlation, InvDfMom: inverse difference moment, SumEntrp: sum of entropy; SumOfSqs: sum of squares ShrtREmp: short run emphasis, GLevNonU: gray level non-uniformity, LngREmph: long run emphasis, RLNonUni: run-length non-uniformity, Horzl: horizontal, Vertl: vertical

relation (S(1.0), S(0.1), S(2.0) and S(3.0)), sum of squares (all positions), sum of entropy (all positions), and entropy (S(0.3)).

Discussion

Computed tomography (CT) plays an important role in the identification of sinus alterations, such as sinusitis or rhinosinusitis, and is considered the gold standard complementary examination for pathological conditions in the paranasal sinus. In this context, it is essential to distinguish between possible causes of sinus alterations so that an effective treatment plan can be created and a favorable prognosis can be achieved.[2,4]

The differential diagnosis between OS and NOS is an important objective of CT, as the pathophysiology and microbiology are quite specific in cases of OS, leading to the need for differentiated management.[1]

In particular, CBCT examinations have been playing an increasingly important role in diagnostic imaging in dental practice and often in otolaryngology because CBCT provides a lower radiation dose than multi-slice tomography. Moreover, CBCT enables high-definition images of mineralized tissues and allows them to be recorded, which makes it possible to identify soft tissue density contents when present, as in sinusitis.[1,3]

This study combined 2 methodologies (i.e., TA of CBCT images) for differentiating between OS and NOS. Initially, it was observed that there were statistically significant differences between the OS and NOS groups regarding the con-

trast parameter (Table 1) as the highest values were found in cases of NOS. This finding indicates that in images corresponding to NOS, there was a greater lack of uniformity and a greater presence of noise than in those corresponding to OS.

According to Haralick et al.,[25] images with high contrast signify that there is an intensity difference between neighboring regions with noise and lack of uniformity, indicating heterogeneity and asynchronous behavior in the pixel pattern.

In accordance with this finding, the present results also showed that in addition to contrast, 2 other texture parameters had statistically significant differences between the groups, namely: correlation and moment of inverse difference.

Initially, it was observed that the correlation parameter showed a statistically significant difference between the OS and NOS groups in all positions of the pixel distributions, thus being quite representative, as the former had higher correlation values than the latter. In TA using GLCM, the correlation between pixels of the matrix is expected to be high when gray levels of the image between each pixel pair are highly correlated. This parameter provides the correlation of a pixel with its neighbors throughout the image and its linear interdependence.[18,24] A high linear interdependence (i.e., higher correlation values) can indicate a greater uniformity in the image behavior, which occurred in the OS group. This association with lower contrast values in this group, as already mentioned, indicates that the tissue corresponding to OS would be more standardized from a mathematical point of view; that is, the formation of mucus in OS would have a pattern. This can be explained by the fact that the most common cause of OS is apical periodontitis,[26,27] which involves the action of specific microorganisms. In contrast, NOS can have a greater range of etiological factors, such as fungi, bacteria, and allergens, among others, which would make images of NOS less homogeneous concerning OS.

The other parameter showing a statistically significant difference between the 2 groups was the inverse difference moment, as the OS group had higher values than the NOS group. This parameter is directly linked to the smoothness (homogeneity) of the distribution of gray levels in the image, and according to Haralick et al.,[25] when the contrast value is low, the value of the inverse difference moment becomes high. This relationship can be observed in these results, as the OS group had lower values of contrast than the NOS group. This result further reinforces the tissue homogeneity behavior in images of OS, corroborating a previous study[4] using TA to investigate the difference between OS and NOS on multi-slice CT.

Concerning the parameters related to GLRLM, differences between the NOS and OS groups were found in run-length non-uniformity and gray level non-uniformity in both horizontal and vertical directions, with the former group having values higher than those of the latter group. This finding underscores that the uniformity of pixel values corresponding to OS were greater than that of pixel values corresponding to NOS, thus indicating a more standardized behavior, as mentioned above. TA using GLRLM made it possible to confirm this behavior after the use of GLCM, functioning as a double-check.

In a comparison of the dispersion of the variables (standard deviation values) between the groups, it was observed that the OS group had lower values of standard deviations for each variable studied in all directions, reflecting the more homogeneous pixel values. Statistically significant differences were found between groups in the standard deviations for correlation (which is contrary to the previously presented findings), sum of squares, sum of entropy, and entropy.

These findings further emphasize what had already been observed concerning a more regular pattern of images in the OS group. The sum of squares, sum of entropy, and entropy are parameters that represent the measurement of the dispersion of gray-level distribution.[25] The images of OS had smaller dispersions of gray value pixels than the images of NOS, thus indicating uniformity. The dispersion of the entropy parameter, with lower standard deviations in the OS group, also indicates less disarray among the pixels in the image[21,22,28] than in the NOS group.

A recent study[4] investigated the role of TA in differentiating between OS and NOS and showed that this technique provided values enabling a quantitative differentiation, similar to the results of the present study. However, in that study, the authors used examinations obtained through multi-slice CT, which is known to provide a higher dose of radiation than CBCT. Thus, this study presents a basis for validating the use of TA in CBCT for this purpose, also considering that the results found herein regarding TA values are quite similar to those of the aforementioned study.

This fact is very important because professionals who handle findings related to sinusitis, mostly dentists, need to differentiate between OS and NOS, and this undoubtedly requires the use of CBCT[29] instead of multi-slice CT examinations in daily practice, such as implant planning and sinus surgery, which can be directly related to the presence of sinusitis.

It is also important to mention that this study has some limitations, such as the number of CBCT exams in the sample in each group. However, compared to the study by Ito et al.,[4] this sample is superior, as 20 CBCT exams were used per group. Another limitation is the fact that the phases of sinusitis were not considered, which may be an objective of further studies. An additional limitation was that none of the cases had a histologically confirmed diagnosis.

In conclusion, the results indicated that TA allowed a quantitative differentiation between OS and NOS on CBCT images by using the parameters of contrast, correlation, and inverse moment of difference, with the OS images presenting more homogeneous behavior regarding texture parameters than the NOS images.

Conflicts of Interest: None

References

1. Nair UP, Nair MK. Maxillary sinusitis of odontogenic origin: cone-beam volumetric computerized tomography-aided diagnosis. Oral Surg Oral Med Oral Pathol Oral Radiol Endod 2010; 110: e53-7.
2. Maillet M, Bowles WR, McClanahan SL, John MT, Ahmad M. Cone-beam computed tomography evaluation of maxillary sinusitis. J Endod 2011; 37: 753-7.
3. Longhini AB, Branstetter BF, Ferguson BJ. Radiology quiz case 1. Acute maxillary sinusitis secondary to a migrated dental implant obstructing the ostiomeatal complex. Arch Otolaryngol Head Neck Surg 2011; 137: 823, 826.
4. Ito K, Kondo T, Andreu-Arasa VC, Li B, Hirahara N, Muraoka H, et al. Quantitative assessment of the maxillary sinusitis using computed tomography texture analysis: odontogenic vs non-odontogenic etiology. Oral Radiol 2022; 38: 315-24.
5. Tsuzuki K, Kuroda K, Hashimoto K, Okazaki K, Noguchi K, Kishimoto H, et al. Odontogenic chronic rhinosinusitis patients undergoing tooth extraction: oral surgeon and otolaryngologist viewpoints and appropriate management. J Laryngol Otol 2020; 134: 241-6.
6. Parks ET. Cone beam computed tomography for the nasal cavity and paranasal sinuses. Dent Clin North Am 2014; 58: 627-51.
7. Ritter L, Lutz J, Neugebauer J, Scheer M, Dreiseidler T, Zinser MJ, et al. Prevalence of pathologic findings in the maxillary sinus in cone-beam computerized tomography. Oral Surg Oral Med Oral Pathol Oral Radiol Endod 2011; 111: 634-40.
8. Abrahams JJ, Glassberg RM. Dental disease: a frequently unrecognized cause of maxillary sinus abnormalities? AJR Am J Roentgenol 1996; 166: 1219-23.
9. Zhu J, Lin W, Yuan W, Chen L. New insight on pathophysiology, diagnosis, and treatment of odontogenic maxillary sinusitis. J Nanomater 2021; 2021: 9997180.
10. Shen Q, Shan Y, Hu Z, Chen W, Yang B, Han J, et al. Quantitative parameters of CT texture analysis as potential markersfor early prediction of spontaneous intracranial hemorrhage enlargement. Eur Radiol 2018; 28: 4389-96.
11. Mungai F, Verrone GB, Pietragalla M, Berti V, Addeo G, Desideri I, et al. CT assessment of tumor heterogeneity and the potential for the prediction of human papillomavirus status in oropharyngeal squamous cell carcinoma. Radiol Med 2019; 124: 804-11.
12. Tsai A, Buch K, Fujita A, Qureshi MM, Kuno H, Chapman MN, et al. Using CT texture analysis to differentiate between nasopharyngeal carcinoma and age-matched adenoid controls. Eur J Radiol 2018; 108: 208-14.
13. De Rosa CS, Bergamini ML, Palmieri M, Sarmento DJ, de Carvalho MO, Ricardo AL, et al. Differentiation of periapical granuloma from radicular cyst using cone beam computed tomography images texture analysis. Heliyon 2020; 6: e05194.
14. Lubner MG, Smith AD, Sandrasegaran K, Sahani DV, Pickhardt PJ. CT texture analysis: definitions, applications, biologic correlates, and challenges. Radiographics 2017; 37: 1483-503.
15. Larroza A, Moratal D, Paredes-Sánchez A, Soria-Olivas E, Chust ML, Arribas LA, et al. Support vector machine classification of brain metastasis and radiation necrosis based on texture analysis in MRI. J Magn Reson Imaging 2015; 42: 1362-8.
16. Castellano G, Bonilha L, Li LM, Cendes F. Texture analysis of medical images. Clin Radiol 2004; 59: 1061-9.
17. Huang YH, Chang YC, Huang CS, Wu TJ, Chen JH, Chang RF. Computer-aided diagnosis of mass-like lesion in breast MRI: differential analysis of the 3-D morphology between benign and malignant tumors. Comput Methods Programs Biomed 2013; 112: 508-17.
18. Buch K, Fujita A, Li B, Kawashima Y, Qureshi MM, Sakai O. Using texture analysis to determine human papillomavirus status of oropharyngeal squamous cell carcinomas on CT. AJNR Am J Neuroradiol 2015; 36: 1343-8.
19. Raja JV, Khan M, Ramachandra VK, Al-Kadi O. Texture analysis of CT images in the characterization of oral cancers involving buccal mucosa. Dentomaxillofac Radiol 2012; 41: 475-80.
20. Obuchowicz R, Nurzynska K, Obuchowicz B, Urbanik A, Piórkowski A. Caries detection enhancement using texture feature maps of intraoral radiographs. Oral Radiol 2020; 36: 275-87.
21. Gonçalves BC, de Araújo EC, Nussi AD, Bechara N, Sarmento D, Oliveira MS, et al. Texture analysis of cone-beam computed tomography images assists the detection of furcal lesion. J Periodontol 2020; 91: 1159-66.
22. Costa AL, de Souza Carreira B, Fardim KA, Nussi AD, da Silva Lima VC, Miguel MM, et al. Texture analysis of cone beam computed tomography images reveals dental implant stability. Int J Oral Maxillofac Surg 2021; 50: 1609-16.
23. Galloway MM. Texture analysis using gray level run lengths. Comput Graph Image Process 1975; 4: 172-9.
24. Whyte A, Boeddinghaus R. Imaging of odontogenic sinusitis. Clin Radiol 2019; 74: 503-16.
25. Haralick RM, Shanmugam K, Dinstein I. Textural features for image classification. IEEE Trans Syst Man Cybern 1973; 3: 610-21.
26. Tonetti MS, Greenwell H, Kornman KS. Staging and grading of periodontitis: framework and proposal of a new classification and case definition. J Periodontol 2018; 89 Suppl 1: S159-72.
27. Simuntis R, Kubilius R, Vaitkus S. Odontogenic maxillary sinus-

itis: a review. Stomatologija 2014; 16: 39-43.
28. Fujimoto K, Tonan T, Azuma S, Kage M, Nakashima O, Johkoh T, et al. Evaluation of the mean and entropy of apparent diffusion coefficient values in chronic hepatitis C: correlation with pathologic fibrosis stage and inflammatory activity grade. Radiology 2011; 258: 739-48.
29. Aksoy U, Orhan K. Association between odontogenic conditions and maxillary sinus mucosal thickening: a retrospective CBCT study. Clin Oral Investig 2019; 23: 123-31.